

Geographic and temporal variations in turbulent heat loss from lakes: a global analysis across 45 lakes

Article

Accepted Version

Woolway, R. I. ORCID: <https://orcid.org/0000-0003-0498-7968>, Verburg, P., Lenters, J. D., Merchant, C. J. ORCID: <https://orcid.org/0000-0003-4687-9850>, Hamilton, D. P., Brookes, J., de Eyto, E., Kelly, S., Healey, N. C., Hook, S., Laas, A., Pierson, D., Rusak, J. A., Kuha, J., Karjalainen, J., Kallio, K., Lepisto, A. and Jones, I. D. (2018) Geographic and temporal variations in turbulent heat loss from lakes: a global analysis across 45 lakes. *Limnology and Oceanography*, 63 (6). pp. 2436-2449. ISSN 0024-3590 doi: 10.1002/lno.10950 Available at <https://centaur.reading.ac.uk/77266/>

It is advisable to refer to the publisher's version if you intend to cite from the work. See [Guidance on citing](#).

To link to this article DOI: <http://dx.doi.org/10.1002/lno.10950>

Publisher: Wiley

All outputs in CentAUR are protected by Intellectual Property Rights law, including copyright law. Copyright and IPR is retained by the creators or other copyright holders. Terms and conditions for use of this material are defined in

the [End User Agreement](#).

www.reading.ac.uk/centaur

CentAUR

Central Archive at the University of Reading

Reading's research outputs online

1 **Title**

2 Geographic and temporal variations in turbulent heat loss from lakes: A global analysis
3 across 45 lakes

4

5 **Author information**

6 R. Iestyn Woolway^{1*}, Piet Verburg², John D. Lenters³, Christopher J. Merchant^{1,4}, David P.
7 Hamilton⁵, Justin Brookes⁶, Elvira de Eyto⁷, Sean Kelly^{7,8}, Nathan C. Healey⁹, Simon Hook⁹,
8 Alo Laas¹⁰, Don Pierson¹¹, James A. Rusak¹², Jonna Kuha¹³, Juha Karjalainen¹³, Kari
9 Kallio¹⁴, Ahti Lepistö¹⁴, Ian D. Jones¹⁵

10

11 **Affiliation**

- 12 1. *Department of Meteorology, University of Reading, Reading, UK*
- 13 2. *National Institute of Water and Atmospheric Research, Hamilton, New Zealand*
- 14 3. *Center for Limnology, University of Wisconsin-Madison, USA*
- 15 4. *National Centre for Earth Observation, University of Reading, Reading, UK*
- 16 5. *Australian Rivers Institute, Griffith University, Brisbane, Australia*
- 17 6. *The Environment Institute, School of Biological Sciences, University of Adelaide,*
18 *Australia*
- 19 7. *Marine Institute, Furnace, Newport, Co Mayo, Ireland*
- 20 8. *Earth & Ocean Science, School of Natural Sciences, National University of Ireland*
21 *Galway, Galway, Ireland*
- 22 9. *Jet Propulsion Laboratory, California Institute of Technology, Pasadena, California,*
23 *USA*
- 24 10. *Estonian University of Life Sciences, Institute of Agricultural and Environmental*
25 *Sciences, Centre for Limnology, Tartu, Kreutzwaldi 5D, Estonia*
- 26 11. *Department of Ecology and Genetics/Limnology, Uppsala University, Uppsala,*
27 *Sweden*
- 28 12. *Dorset Environmental Science Centre, Ontario Ministry of the Environment and*
29 *Climate Change, Dorset, ON Canada*
- 30 13. *Department of Biological and Environmental Science, University of Jyväskylä,*
31 *Jyväskylä, Finland*
- 32 14. *Finnish Environment Institute, Helsinki, Finland*
- 33 15. *Centre for Ecology & Hydrology, Lancaster Environment Centre, Lancaster, UK*

34

35 *Corresponding author; email: riwoolway@gmail.com

36

37 **Abstract**

38 Heat fluxes at the lake surface play an integral part in determining the energy budget and
39 thermal structure in lakes, including regulating how lakes respond to climate change. We
40 explore patterns in turbulent heat fluxes, which vary across temporal and spatial scales, using
41 in situ high-frequency monitoring data from 45 globally distributed lakes. Our analysis
42 demonstrates that some of the lakes studied follow a marked seasonal cycle in their turbulent
43 surface fluxes, and that turbulent heat loss is highest in larger lakes and those situated at low
44 latitude. The Bowen ratio, which is the ratio of mean sensible to mean latent heat fluxes, is

45 smaller at low latitudes and, in turn, the relative contribution of evaporative to total turbulent
46 heat loss increases towards the tropics. Latent heat transfer ranged from ~60 to >90% of total
47 turbulent heat loss in the examined lakes. The Bowen ratio ranged from 0.04 to 0.69 and
48 correlated significantly with latitude. The relative contributions to total turbulent heat loss
49 therefore differ among lakes and these contributions are influenced greatly by lake location.
50 Our findings have implications for understanding the role of lakes in the climate system,
51 effects on the lake water balance, and temperature-dependent processes in lakes.

52

53 **Introduction**

54 Wind stress and surface heating/cooling are two of the more important factors driving
55 physical processes within lakes (Wüest and Lorke 2003), wherein water movements forced
56 by the wind produce turbulent mixing that combines with surface heating/cooling to
57 determine the physical environment of the lake ecosystem. Lake thermal structure regulates
58 key aspects of lake ecosystems and is influenced by the interactions between the lake surface
59 and the overlying atmosphere (Edinger et al. 1968). Some of the most important physical
60 effects of climate change on the physics, chemistry, and biology of lakes (De Stasio et al.
61 1996) are associated with changes in thermal structure, heat budgets, and ultimately the
62 fluxes of heat and energy at the air-water interface (McCormick 1990; Livingstone 2003;
63 Fink et al. 2014; Schmid et al. 2014).

64 By modifying the key processes of mixing and stratification (Peeters et al. 2002;
65 Perroud and Goyette 2010; Stainsby et al. 2011), climate-driven modulation of surface heat
66 fluxes can alter key aspects of lake ecosystems, such as an increased occurrence of toxic
67 cyanobacterial blooms (Jöhnk et al. 2008), deep-water hypoxia (Jankowski et al. 2006; North
68 et al. 2014), and changes in lake productivity (Verburg et al. 2003; O'Beirne et al. 2017).
69 Evaporative heat fluxes also alter lake levels (Gronewold and Stow 2014), with consequences
70 for water security and supply (Brookes et al. 2014) and, in turn, water management strategies
71 (Vörösmarty et al. 2000; Immerzeel et al. 2010; Vörösmarty et al. 2010).

72 Heat loss at the lake surface can modify the intensity of near-surface turbulence
73 (Imberger 1985; Brubaker 1987; Schladow et al. 2002) and thereby influence the efflux of
74 gases such as carbon dioxide and methane from lakes to the atmosphere (MacIntyre et al.
75 2010; Vachon et al. 2010; Dugan et al. 2016). A detailed understanding of surface heat loss
76 processes is therefore essential given the growing realization of the importance of lakes in the
77 global carbon cycle (Cole et al. 2007; Raymond et al. 2013). Surface energy fluxes from
78 lakes can also influence the climate directly (Bonan 1995; Lofgren 1997; Samuelsson et al.
79 2010; Thiery et al. 2015). The surface fluxes of latent and sensible heat, representing the
80 turbulent exchange of energy between a lake and the atmosphere, are critical components of
81 the global surface energy cycle (Dutra et al. 2010; Le Moigne et al. 2016) and can influence
82 the hydrological cycle (Rouse et al. 2005), which is sensitive to climate change (Wentz et al.
83 2007; Wu et al. 2013).

84 Until recently, in situ high-frequency measurements at the air-water interface that are
85 required to accurately examine patterns in surface heat loss fluxes from lakes (e.g., wind
86 speed, water temperature, air temperature, and relative humidity) were not widely available,
87 thus preventing a consistent and comprehensive comparison across lakes. The recent
88 establishment of scientific networks (e.g., Networking Lake Observatories in Europe,

89 NETLAKE; Global Lake Ecological Observatory Network, GLEON) dedicated to the
90 collaborative analysis of high-frequency lake buoy data has provided opportunities for
91 global-scale analyses to be undertaken (Hamilton et al. 2015; Rose et al. 2016). We collated
92 data from 45 lakes across 5 continents (Fig. 1; Table S1) to examine patterns in turbulent
93 surface heat fluxes (i.e., latent and sensible heat fluxes) and determine how these patterns
94 vary across time, space and different lake attributes, such as latitude and depth. To
95 understand the controls on turbulent heat fluxes, we examine the influence of additional
96 variables that we hypothesize may have an effect, including altitude, lake surface area / wind
97 speed, and lake-air differences in temperature and humidity (Woolway et al. 2017a). We
98 predicted that absolute latitude, which is strongly related to annual mean air temperature and
99 net radiation, would have a strong influence on lake temperature (Straskraba 1980; Piccolroaz
100 et al. 2013) and thus heat fluxes at the air-water interface. Altitude can influence air-water
101 temperature relationships via differential lapse rates (Livingstone et al. 1999), and we thus
102 predicted it would influence the cooling fluxes (Rueda et al. 2007; Verburg and Antenucci
103 2010). We predicted that lake area would be an important predictor of surface energy fluxes
104 given that it regulates surface temperature at diel timescales (Woolway et al. 2016) and
105 thereby surface cooling in lakes and has also been shown as an important predictor of the
106 relative importance of convective vs wind-driven mixing (Read et al. 2012). Finally, lake
107 depth can influence the interactions between a lake and the atmosphere and is often correlated
108 strongly with annual lake heat budgets (Gorham 1964), and so we predicted that depth could
109 also influence the surface energy fluxes.

110

111 **Materials and methods**

112 We collected mostly continuous observations (measurement intervals range from 4 min to 1
113 h) of lake surface temperatures and meteorological conditions from 45 lakes (Fig. 1a),
114 ranging in surface area between 0.005 km² and 32,900 km², in altitude between 0 m above
115 sea level (a.s.l.) and 1,897 m a.s.l., and in latitude between 38.8°S and 72.4°N (Table S1).
116 Instrumented buoys measured near-surface water temperature (T_o , °C) at an average depth of
117 approximately 0.5 m (range 0 to 1 m), always within the surface mixed layer. Meteorological
118 conditions including wind speed (U_z , m s⁻¹), air temperature (T_z , °C), and relative humidity
119 (RH , %) were measured on average $z = 2.9$ m (range 1.3 to 10 m) above the lake surface.
120 Fourteen lakes had observations available throughout at least one year. All lakes had
121 observations for the months of July to September (January to March in the Southern
122 Hemisphere) for at least one year. Note that lake variables were not measured annually in
123 some lakes as a result of the monitoring stations being removed prior to the formation of ice
124 cover in winter. Throughout the text we refer to July to September (January to March in the
125 Southern Hemisphere) as ‘summer,’ in-line with previous studies (Woolway et al. 2017a).
126 Each lake had measurements taken at a single location, except for Lake Tanganyika (two
127 locations) and Lake Tahoe (four locations). We analyzed the data independently from each
128 monitoring station in Lakes Tanganyika and Tahoe before combining the results in our
129 statistical analyses (see below). Specifically, for lakes with more than one monitoring station,
130 we calculated the surface heat fluxes (see below) for each site individually and then
131 calculated a lake-wide average.

132 This paper focuses on sensible (Q_h) and latent (Q_e) heat fluxes at the lake surface,
 133 each of which is positive when the direction of heat transfer is from the lake to the
 134 atmosphere (i.e., during surface cooling). The turbulent fluxes, Q_h and Q_e , were calculated as:

$$135 \quad Q_h = \rho_a C_{pa} C_h U_z (T_o - T_z), \quad (1)$$

$$136 \quad Q_e = \rho_a L_v C_e U_z (q_s - q_z), \quad (2)$$

137 where ρ_a is air density (kg m^{-3}), estimated as a function of air pressure, air temperature, and
 138 humidity (Chow et al. 1988; Verburg and Antenucci 2010), $C_{pa} = 1005 \text{ J kg}^{-1} \text{ }^\circ\text{C}^{-1}$ is the
 139 specific heat of dry air at constant pressure, C_h and C_e are the transfer coefficients for heat
 140 and humidity, which were assumed to be equal and adjusted for atmospheric boundary layer
 141 stability, measurement height, and wind speed (at z m above the lake surface) by following
 142 the computational method of Verburg and Antenucci (2010), and

$$143 \quad L_v = 2.501 \times 10^6 - 2370T_o \quad (3)$$

144 is the latent heat of vaporization (J kg^{-1}).

145 The humidity difference, $q_s - q_z$, which influences evaporative heat transfer at the air-
 146 water interface, was calculated as the difference between the specific humidity of saturated
 147 air at the water surface temperature, q_s (kg kg^{-1}):

$$148 \quad q_s = 0.622 e_{sat} / p, \quad (4)$$

149 and the specific humidity of unsaturated air at the measurement height, q_z (kg kg^{-1}):

$$150 \quad q_z = 0.622 e_a / p, \quad (5)$$

151 where e_{sat} is the saturated vapor pressure at T_o (mbar), calculated as:

$$152 \quad e_{sat} = 6.11 \exp^{[17.27T_o / (237.3 + T_o)]} \quad (6)$$

153 and e_a is the vapor pressure (mbar), calculated as:

$$154 \quad e_a = RH e_s / 100, \quad (7)$$

155 with e_s , the saturated vapor pressure at T_z (mbar), calculated as:

$$156 \quad e_s = 6.11 \exp^{[17.27T_z / (237.3 + T_z)]}, \quad (8)$$

157 and RH is relative humidity (%), and p is air pressure (mbar).

158 In this study we also calculate the Bowen ratio (B), which is commonly used with the
 159 energy budget method to estimate evaporation rates in lakes and reservoirs (Gibson et al.
 160 1996; Lenters et al. 2005; Riveros-Iregui et al. 2017) and is defined as the ratio of mean Q_h to
 161 mean Q_e as:

$$162 \quad B = Q_h / Q_e. \quad (9)$$

163 We also calculate the relative contribution of evaporation to the total turbulent heat flux,
 164 referred to hereafter as the evaporative fraction (EF), as:

$$165 \quad EF = Q_e / (Q_h + Q_e) = 1 / (1 + B). \quad (10)$$

166 As air pressure was not measured on all instrumented buoys, and since local
 167 variability in air pressure has a negligible effect on the turbulent fluxes (Verburg and
 168 Antenucci 2010), a constant air pressure was assumed for each lake in this study, calculated
 169 based on the altitude of the lake (Woolway et al. 2015a). With the exception of air pressure,
 170 all data used to estimate the turbulent surface fluxes were measured directly above the lake
 171 surfaces, as opposed to over land. The latter approach was formerly used to be more common
 172 in limnology (Derecki 1981; Croley 1989; Lofgren and Zhu 2000) but has often been shown
 173 to cause large errors (Croley 1989), perhaps contributing to annual mean net surface fluxes
 174 that differ substantially from zero (Lofgren and Zhu 2000).

175 To understand the drivers of variations in turbulent heat fluxes among lakes, we
176 modeled the summer and (where available) annual mean fluxes, calculated from the raw,
177 high-resolution data, against lake attributes using a multiple linear regression model.
178 Latitude, altitude, lake surface area, and depth were used as predictors in each multiple linear
179 regression model evaluated in this study. Altitude and latitude are proxies for climatic
180 variables (e.g., annual mean temperature and/or net radiation). Thus, we are not attempting to
181 comprehensively isolate the ultimate climatic drivers of surface heat fluxes in this study, but
182 to identify patterns that would be of utility for simple geographic models.

183 All statistical analyses in this study were performed in R (R Development Core Team
184 2014). As the height of air temperature and relative humidity measurement varied among the
185 lakes, we converted T_z and q_z to a surface elevation of 10 m (T_{10} and q_{10}) prior to performing
186 comparisons among lakes (Woolway et al. 2015a). Similarly, in the across-lake comparisons,
187 surface wind speed was adjusted to a height of 10 m (u_{10}) following the methods of Woolway
188 et al. (2015a).

189

190 **Results**

191 *Seasonal and diel cycles in turbulent surface fluxes* - Many of the lakes investigated
192 in this study followed a distinct seasonal cycle in their turbulent surface cooling terms (Fig. 2;
193 Fig. 3), albeit less pronounced over, or even absent, in tropical lakes (Fig. 2), where the
194 turbulent fluxes demonstrate near-constant monthly mean values (e.g., Corumba). The latent
195 heat flux (Q_e), and also the sum of the turbulent fluxes (Q_e+Q_h), followed a clear seasonal
196 cycle in many lakes, especially those situated in temperate regions, being highest in summer
197 as a result of a greater air-water humidity difference (Fig. 3a, 3b). The sensible heat flux (Q_h)
198 followed a less pronounced seasonal cycle among all lakes but was, on average, highest in
199 autumn as a result of a greater air-water temperature difference (Fig. 3a, 3c). Specifically, the
200 surface temperatures of lakes typically retain summertime heat well into autumn, resulting in
201 a larger air-water temperature difference at this time of year. This is particularly the case for
202 deep, mid-latitude lakes such as Tahoe (California/Nevada, USA; max. depth = 501m) and
203 Taupo (New Zealand; max. depth = 186m), which experience highest turbulent heat fluxes
204 well into autumn and winter as a result of their greater heat storage capacity. This also results
205 in a higher Bowen ratio ($B = Q_h/Q_e$) in late autumn and winter (Fig. S1). The variation in
206 surface wind speed, u_{10} , which was highest in winter, did not co-vary strongly with Q_e , Q_h , or
207 Q_e+Q_h at seasonal timescales (Fig. 3d).

208 The sensible and latent heat fluxes generally follow a clear diel cycle in summer, but
209 the mean diel cycles are out-of-phase with each other, resulting in a minimal diel cycle in the
210 sum of the turbulent fluxes (Fig. 4a) but considerable diel variability in B (Fig. S2). Q_e is
211 highest during mid-afternoon and lowest during late evening and early morning hours as a
212 result of the diel cycles in wind speed (Fig. 4d) and the humidity difference (Fig. 4b) at the
213 air-water interface (see equation 2), both of which are highest during mid-afternoon. Sensible
214 heat flux follows an opposite diel cycle, with highest Q_h during the late evening and early
215 morning hours, as a result of a greater air-water temperature difference during that time of
216 day (Fig. 4c). Air temperatures above the lake surface tend to be cooler during the evening
217 while the surface water temperatures retain daytime heat longer, resulting in a larger
218 temperature difference. Interestingly, the diel cycle in Q_h is opposite to that of u_{10} , to which

219 Q_h is related (see equation 1). This illustrates that the air-water temperature difference in the
220 studied lakes is the main driver of the diel variability of Q_h , and that the magnitude of the air-
221 water temperature difference outweighs the opposite influence of u_{10} at diel timescales.

222 *Relationships between surface fluxes and lake attributes* - A multiple linear regression
223 model including latitude, altitude, lake surface area, and depth demonstrates a statistically
224 significant ($p < 0.05$) effect of lake surface area and latitude on Q_e during summer and
225 annually (Table S2). Q_e was higher in larger lakes (Fig. 5a; Table S2) and in lakes situated at
226 low latitudes (Fig. 7a; Table S2). Lake surface area also had a statistically significant ($p <$
227 0.05) relationship with Q_h (Fig. 5b) within the multiple linear regression model, with Q_h
228 typically being higher in larger lakes during summer but not annually (Table S2). The
229 relationship between lake surface area and both Q_e and Q_h was not always statistically
230 significant when computing the linear regression within specific climatic zones, but this was
231 primarily a result of the limited number of lakes with available data in some climatic regions
232 (e.g., $n = 8$ in the tropics; $n = 7$ in polar regions).

233 The relationship between lake size and both Q_e and Q_h is explained, in part, by the
234 lake-size dependence in over-lake wind speed. Larger lakes with greater fetch typically
235 experience higher wind speeds (Fig. 5c), via the acceleration of wind over water. In the lakes
236 studied, there was a statistically significant positive linear relationship between lake size and
237 u_{10} during summer ($r^2 = 0.23$, $p < 0.001$, $n = 45$) but not with latitude or altitude ($p > 0.1$),
238 thus suggesting an effect of lake fetch. However, we must note that the linear lake-size
239 dependence in u_{10} is not likely to extend indefinitely to the world's largest lakes, since once a
240 lake reaches a certain (unknown) size threshold, the atmospheric boundary layer has
241 essentially adjusted to the lake surface area, and so any further increases in lake size would
242 not lead to further increases in over-lake wind speed.

243 The relationship of lake size and u_{10} results in greater Q_h and Q_e (equations 1 and 2) in
244 the lakes studied. However, Q_h and Q_e are also influenced by the air-water temperature and
245 humidity differences, respectively and, thus the lake-size dependence of these differences
246 must also be considered. There is no statistically significant lake-size dependence in the air-
247 water humidity difference ($r^2 = 0.04$, $p = 0.17$, $n = 45$), to which Q_e is related, in the studied
248 lakes. However, we calculate a significant negative relationship between lake size and $T_o -$
249 T_{10} ($r^2 = 0.16$; $p < 0.05$, $n = 45$), with a greater temperature difference in smaller lakes (Fig.
250 5d). Therefore, the influence of lake size on $T_o - T_{10}$, to which Q_h is related, is opposite to that
251 of u_{10} , resulting in the relationship between lake size and Q_h being weaker than the observed
252 relationship between lake size and Q_e (Table S2).

253 *Relative contributions to total turbulent heat loss* - In terms of the total turbulent heat
254 fluxes ($Q_h + Q_e$), a multiple linear regression model (testing the influence of latitude, altitude,
255 lake surface area, and lake depth) demonstrates that latitude and lake surface area are
256 statistically significant predictors (Table S3). More total turbulent heat loss was found in
257 lakes with greater surface area (Fig. 6) and for lakes situated at low latitude (Fig. 7c). In
258 contrast to the diel cycle, which shows an out-of-phase covariance between Q_h and Q_e (Fig.
259 4a), lakes often show in-phase covariance on seasonal timescales (Fig. 3a). The magnitude of
260 these turbulent fluxes, however, can differ considerably among lakes. The ratio of Q_h to Q_e
261 (i.e., the Bowen ratio) demonstrates that Q_h is consistently lower than Q_e (Fig. 7d), with an
262 average $B (= Q_h/Q_e)$ across all lakes of 0.23 (± 0.11 std. dev.) during summer ($n = 45$). Fitting

263 a multiple linear regression model (testing the influence of latitude, altitude, lake surface
264 area, and lake depth) demonstrates that latitude is the only statistically significant ($p < 0.05$)
265 predictor of B (Table S4). Thus, during summer and across the year B is lower at lower
266 latitude, as a result of Q_e , but not Q_h , increasing with decreasing latitude (Fig. 7; Table S2).
267 As would be expected, the relevant contribution of Q_e to total turbulent heat loss, in turn,
268 increases towards the tropics (Fig. 7d). Specifically, Q_e can contribute $>90\%$ of the total
269 turbulent heat exchange in some lakes during summer (Fig. 7d). The contribution of Q_h to
270 total turbulent heat exchange increases at higher latitude, where summer Q_h can contribute
271 approximately 40% of the total turbulent heat exchange. Given the lack of year-round data
272 for many of the lakes in this study, it is important to note that – particularly for deep lakes in
273 mid-latitudes – significantly higher Q_h , and therefore B , can occur in late autumn and into
274 winter (Fig. 3; Fig. S1).

275 The decrease in B with decreasing latitude is a result of the Clausius-Clapeyron
276 relationship, with Q_e higher in warmer lakes situated in warmer climates. To explain the
277 effect of latitude on Q_e (Fig. 7a), but not Q_h (Fig. 7b), we compared, across lakes, the
278 humidity and temperature differences at the air-water interface, to which Q_e and Q_h are
279 respectively proportional. With decreasing latitude, we calculated a rapid and statistically
280 significant ($p < 0.05$) increase in q_s , q_{10} , T_o , and T_{10} (Fig. 8). We find no relationship of
281 latitude to the air-water temperature difference in these lakes ($T_o - T_{10}$), while there was a
282 statistically significant increase in the humidity difference ($q_s - q_{10}$) with decreasing latitude.
283 The latter results from the non-linearity of the Clausius-Clapeyron relationship and the
284 resulting dependence of vapor pressure difference on temperature (equations 6 - 8), which is
285 strongly related to absolute latitude both annually ($r^2 = 0.89$, $p < 0.001$) and during summer
286 ($r^2 = 0.79$, $p < 0.001$). Thus, at low latitudes, $q_s - q_{10}$ will be greater, resulting in higher Q_e and
287 lower B .

288

289 Discussion

290 We investigated the differences in turbulent surface heat fluxes from 45 lakes across five
291 continents. These turbulent fluxes have been investigated in lakes around the world for many
292 years (Dutton and Bryson 1962; Lofgren and Zhu 2000; MacIntyre et al. 2002; Momii and Ito
293 2008), but our study is the first, to our knowledge, to investigate and compare these fluxes
294 across a range of climatic zones and lake attributes. In addition, many earlier studies that
295 have calculated surface heat fluxes from lakes have used remotely sensed water temperature
296 in combination with land-based meteorological measurements (Derecki 1981; Croley 1989;
297 Lofgren and Zhu 2000) or reanalysis data (Moukomla and Blanken 2017), which can lead to
298 erroneous estimates of air-water interactions. Studies that have calculated heat fluxes using in
299 situ temperature and meteorology data have dealt primarily with single lakes (Laird and
300 Kristovich 2002; MacIntyre et al. 2002; Lenters et al. 2005; Verburg and Antenucci 2010;
301 Lorenzetti et al. 2015; Dias and Vissotto 2017), or a number of lakes from a confined region
302 (Woolway et al. 2015b). Prior to this investigation, no known previous studies have
303 compared turbulent surface fluxes from continuously recorded buoy data at so many lakes
304 across the globe, and at diel, seasonal, and annual timescales.

305 Using in situ observations from 45 lakes, we show that the turbulent surface fluxes of
306 latent and sensible heat and their relative contributions to total turbulent heat loss at the air-

307 water interface can vary considerably across temporal and spatial scales. Our analysis
308 demonstrates that latent and sensible heat fluxes follow a pronounced diel cycle in summer
309 and, for lakes with data available throughout the year, follow a predictable seasonal cycle in
310 small to medium-sized temperate lakes, with high Q_e , Q_h , and $Q_e + Q_h$ in summer (later in the
311 year for deeper lakes). In tropical lakes the turbulent surface fluxes follow a less pronounced
312 seasonal cycle, but rather experience comparatively high turbulent heat loss throughout the
313 year, which is expected given the increase in heat gain towards the equator (Verburg and
314 Antenucci 2010; Woolway et al., 2017a). The reduced seasonality of the lake heat content
315 (the difference between minimum and maximum heat content) towards the equator
316 demonstrates that heating and cooling are more separated by season at higher latitudes,
317 resulting in a greater amplitude of the heat budget. In deep and large temperate lakes, such as
318 Tahoe and Taupo, the turbulent energy fluxes are greatest during autumn and winter, as a
319 result of the large heat capacity that causes their surface waters to cool more slowly during
320 winter than the ambient surface air, as has been reported in other studies focusing on large,
321 deep North American lakes (Blanken et al. 2011; Moukomla and Blanken 2017). These
322 results indicate that the season in which the turbulent surface energy fluxes from lakes
323 interact most strongly with the overlying atmosphere (and also affect internal lake mixing
324 processes) can vary considerably among lakes.

325 A comparison across lakes of the relative contributions of Q_h and Q_e to the total
326 turbulent heat flux demonstrates interesting relationships. The Bowen ratio ($B = Q_h/Q_e$) is
327 found to decrease toward the tropics, since Q_e increases with decreasing latitude (i.e.,
328 increasing lake surface temperature), while Q_h does not. B is lower in a warmer climate, both
329 in summer and annually. Similar to lakes at low latitude, one might also expect that Q_e would
330 vary with altitude, as a result of the decrease in air temperature with increasing altitude and
331 the temperature dependence of the specific humidity differences (for a given relative
332 humidity). Specifically, we would expect an altitudinal dependence of Q_e and also B in the
333 studied lakes. However, our global-scale analysis demonstrated that altitude did not have a
334 statistically significant effect when investigated alongside latitude, lake surface area, and
335 depth. Latitude was the only statistically significant predictor of B . In turn, the relevant
336 contribution of Q_e to total turbulent heat loss is greater in tropical lakes (upwards of 90%)
337 and then decreases toward higher latitude (~60-70%). While this relationship is expected due
338 to the temperature dependence of specific humidity differences, this study is the first to
339 calculate B across a global sample of lakes using in situ high-resolution data collected at the
340 lake surface. The lowest annual mean B calculated in this study was 0.06 for Lake
341 Tanganyika, while the highest annual mean B was 0.31 for Rotorua. The lowest summer
342 mean B calculated was 0.04 for Lake Tahoe, while the highest summer mean B calculated
343 was 0.69 for Emaiksoun Lake, Alaska, USA. Even higher values of B have been reported on
344 seasonal or shorter timescales in other lake studies. For example, Lenters et al. (2005)
345 calculated a B of 0.85 during early November in Sparkling Lake (Wisconsin, USA), and other
346 studies have demonstrated that B can approach and even exceed 1 for some lakes during
347 winter (Lofgren and Zhu 2000; Blanken et al. 2011), indicating that Q_h can occasionally be
348 larger than Q_e . This highlights the need for continued and expanded analysis of high-
349 frequency heat flux measurements on lakes, particularly during the cold season when such
350 measurements are difficult and infrequently undertaken.

351 Our results, in particular those that illustrate the non-linear functional form of B with
352 latitude, are useful for measuring/predicting the energy balance of lakes globally, since a
353 number of methods (and models) use estimates of B to solve the energy balance and/or to
354 estimate Q_h or Q_e . A constant B is used commonly in, for example, paleoclimate studies and
355 also in simplified lake models (Bultot 1993; Blodgett et al. 1997). Our results demonstrate
356 that a common value of B should not be assumed, and our findings can provide ways of
357 estimating B for lakes as a function of latitude, for example (e.g., in the absence of expensive
358 instrumentation), which can help advance prediction of lake thermal processes. Moreover,
359 our results challenge the validity of neglecting the effect of varying B , which has
360 consequences for estimating lake thermal processes, which are fundamental to understanding
361 lake biogeochemistry and ecology. The proportion of $Q_h:Q_e$ is also important for
362 understanding the influence of climate change on the water balance of lakes and in evaluating
363 the role of lakes in the Earth's hydrologic cycle, which is expected to accelerate with climate
364 change (Wentz et al. 2007; Wu et al. 2013; Wang et al. 2018).

365 While our analysis included observations from lakes across five continents, these
366 were typically restricted to specific years and, as such, may not have captured "normal"
367 meteorological conditions for a particular lake, nor a reasonable range of interannual
368 variability. As such, any lake-to-lake comparisons could have been biased by the presence of
369 'abnormal' years (e.g., drought, flood, heat waves, etc.). For example, one lake may have
370 experienced temperatures above the mean while another lake experienced temperatures below
371 the mean, which could bias our global relationships. Nevertheless, we have found the
372 relationships between the turbulent heat fluxes, in particular with latitude and lake size, to be
373 statistically significant. This occurs despite potential errors in the data and that the 'noise'
374 introduced into the global relationships by any one anomalous lake or anomalous weather
375 during a given year. A caveat to our results regarding the relationship between latitude and
376 the turbulent surface heat fluxes is that not all latitudes are equally represented by study
377 lakes, with fewer or no lakes in areas of critical climate gradients, such as the descending
378 branches of the Hadley cell, which can influence local climate. In addition, latitude serves as
379 a proxy for climatic variables (e.g., air temperature and net radiation) but not completely as
380 factors such as altitude also controls these same variables.

381 Although Q_h is a relatively minor component of total turbulent heat loss in some
382 lakes, contributing ~10% during summer in the tropics, it can be much larger during certain
383 times of the year (and at diel timescales), which could influence greatly convective mixing in
384 a lake and gas transfer at the lake surface. In particular, estimates of carbon dioxide emissions
385 from lakes can be considerably biased when Q_h is not considered (Podgrajsek et al. 2015).
386 Climatic warming will likely increase Q_h in the future, as suggested by the observation that
387 summer-mean water surface temperatures in many lakes have increased more than air
388 temperatures in the past few decades (O'Reilly et al. 2015), thereby increasing the lake-air
389 temperature difference, to which Q_h is proportional. Lake surface temperatures in high
390 latitude lakes, in which Q_h is a relatively large contributor of total turbulent heat loss, have
391 been suggested to experience an amplified response to air temperature variability (Woolway
392 and Merchant 2017). Thus, as a result of the expected increase in Q_h with climate change,
393 there will be a relatively greater increase in total turbulent heat loss at high latitude. Any
394 enhanced lake-air temperature differences induced by climate warming are also likely to be

395 accompanied by enhanced heat loss via Q_e and, in turn, affect gas fluxes into and out of lakes.
396 However, we must note that changes in other meteorological variables associated with the
397 turbulent fluxes, in particular surface wind speed (Woolway et al. 2017b), must also be
398 considered.

399 This large-scale analysis of the spatial and temporal variations in turbulent surface
400 heat flux processes among lakes has implications for carbon dioxide and methane emissions
401 (Polsenaere et al. 2013; Podgrajsek et al. 2015). Previous studies have demonstrated that
402 convective mixing dominates wind-induced mixing in small lakes (Read et al. 2012), and that
403 a simple wind-based approach for estimating the gas transfer coefficient can underestimate
404 lake metabolism and gas exchange with the atmosphere. While our results verify some
405 aspects of this previous work, such as the significantly positive relationship between lake area
406 and wind speeds, we also arrive at some important conclusions regarding the surface cooling
407 processes that lead to convective mixing. For example, we show that turbulent surface
408 cooling (esp. Q_e) is considerably lower in small lakes whereas large lakes have considerably
409 larger Q_e and overall turbulent heat loss. These results indicate that the higher wind speeds
410 that lead to greater wind-induced mixing on large lakes also lead to greater turbulent heat loss
411 and potentially convective mixing, especially during times when such cooling processes are
412 not offset by significant surface radiative heating (e.g., strong incoming solar and thermal
413 radiation). Similarly high rates of Q_e and total turbulent surface heat loss are also found for
414 lakes situated in warmer climates (e.g., tropical lakes). Therefore, our results suggest that
415 convective mixing may be more important in large and tropical lakes than has been suggested
416 previously and that convection may be a greater contributor to gas exchange in these systems
417 as well.

418

419 **Conclusions**

420 We have analyzed high-resolution monitoring data from 45 lakes across 5 continents to study
421 the global variation in mean (summer and annually) turbulent surface heat fluxes at the air-
422 water interface. Our results indicate the relative importance of lake location and lake specific
423 characteristics (e.g., surface area and depth) to the turbulent exchange of heat and energy at
424 the lake surface and also how these fluxes vary at diel, seasonal and annual timescales. We
425 demonstrate that the turbulent fluxes follow predictable diel and seasonal cycles in many
426 lakes, and that, on average, the sum of the turbulent fluxes are greater in larger lakes and in
427 those situated at low latitude. The ratio of mean sensible to mean latent heat fluxes, often
428 referred to as the Bowen ratio and used commonly to estimate evaporation rates in lakes, was
429 shown to vary predictably with latitude, being lower in the tropics. In turn, our study
430 demonstrates that the relative contribution of latent to total turbulent heat loss in lakes varies
431 predictably with latitude. Our results, therefore, demonstrate that the latent and sensible
432 contributions to total turbulent heat loss differ among lakes and these contributions are
433 influenced greatly by lake location. This will be useful for predicting the energy balance of
434 lakes globally, in particular in the absence of expensive instrumentation required to solve the
435 lake energy budget.

436

437 **References**

438 Blanken, P. D., C. Spence, N. Hedstrom, and J. D. Lenters. 2011. Evaporation from Lake
439 Superior: 1. Physical controls and processes. *J. Great Lakes Res.* **37**: 707-716

440 Blodgett, T. A., J. D. Lenters, B. L. Isacks. (1997). Constraints on the Origin of Paleolake
441 Expansions in the Central Andes. *Earth Interactions* **1**: 1-28

442 Bonan, G. B. 1995. Sensitivity of a GCM simulation to inclusion of inland water surfaces. *J.*
443 *Climate* **8**: 2691-2704

444 Brookes, J. D., and others. (2014). Emerging challenges for the drinking water industry.
445 *Environ. Sci. Technol.* **48**: 2099-2101. doi:10.1021/es405606t

446 Brubaker, J. M. 1987. Similarity structure in the convective boundary layer of a lake. *Nature*
447 **330**: 742-745

448 Bultot, F. 1993. Evaporation from a tropical lake: comparison of theory with direct
449 measurements – comment. *Journal of Hydrology* **143**: 513-519

450 Chow, V. T., D. R. Maidment, and L. W. Mays. 1988. Applied hydrology. New York.
451 McGraw-Hill

452 Cole, J. J., and others. 2007. Plumbing the global carbon cycle: Integrating inland waters into
453 the terrestrial carbon budget. *Ecosystems* **10**: 172–185. doi:10.1007/s10021-006-
454 9013-8

455 Croley, T. E. II. 1989. Verifiable evaporation modeling on the Laurentian Great Lakes. *Water*
456 *Resour. Res.* **25**: 781-792. doi:10.1029/WR025i005p00781

457 De Stasio, B. T. Jr., and others. 1996. Potential effects of global climate change on small
458 north-temperate lakes: Physics, fish, and plankton. *Limnol. Oceanogr.* **41**(5): 1136-
459 1149

460 Derecki, J. A. 1981. Stability effects on Great Lakes Evaporation. *J. Great Lakes Res.* **7**: 357-
461 362

462 Dias, N. L., and D. Vissotto. 2017. The effect of temperature-humidity similarity on Bowen
463 ratios, dimensionless standard deviations, and mass transfer coefficients over a lake.
464 *Hydrol. Procces.* **31**: 256-269. doi:10.1002/hyp.10925

465 Dugan, H. A., and others. 2016. Consequences of gas flux model choice on the interpretation
466 of metabolic balance across 15 lakes. *Inland Waters* **6**: 581-591. doi:10.5268/IW-
467 6.4.836

468 Dutra, E., and others. 2010. An offline study of the impact of lakes on the performance of the
469 ECMWF surface scheme. *Boreal Environ. Res.* **15**: 100-112

470 Dutton, J. A., and R. A. Bryson. 1962. Heat flux in Lake Mendota. *Limnol. Oceanogr.* **7**(1):
471 80-97. doi:10.4319/lo.1962.7.1.0080

472 Edinger, J. E., D. W. Duttweiler, and J. C. Geyer. 1968. Response of water temperatures to
473 meteorological conditions. *Water Resour. Res.* **4**: 1137-1143

474 Fink, G., M. Schmid, B. Wahl, T. Wolf, and A. Wüest. 2014. Heat flux modifications related
475 to climate-induced warming of large European lakes. *Water Resour. Res.* **50**: 2072-
476 2085

477 Gibson, J. J., T. D. Prowse, and T. W. D. Edwards. 1996. Evaporation from a small lake in
478 the continental arctic using multiple methods. *Nordic Hydrology* **27**: 1-24

479 Gorham, E. 1964. Morphometric control of annual heat budgets in temperate lakes. *Limnol.*
480 *Oceanogr.* **9**(4): 525-529. doi:10.4319/lo.1964.9.4.0525.

481 Gronewold, A. D., and C. A. Stow. 2014. Water loss from the Great Lakes. *Science*
482 **343**(6175): 1084–1085. doi:10.1126/science.1249978

483 Hamilton, D. P., C. C. Carey, L. Arvola, and others. 2015. A Global Lake Ecological
484 Observatory Network (GLEON) for synthesizing high-frequency sensor data for
485 validation of deterministic models. *Inland Waters* **5**: 49-56

486 Imberger, J. 1985. The diel mixed layer. *Limnol. Oceanogr.* **30**(4): 737-770.
487 doi:10.4319/lo.1985.30.4.0737

488 Immerzeel, W. W., L. P. H. van Beek, and M. F. P. Bierkens. 2010. Climate change will
489 affect the Asian water towers. *Science* **328**(5984): 1382-1385.
490 doi:10.1126/science.1183188

491 Jankowski, T., and others. 2006. Consequences of the 2003 European heat wave for lake
492 temperature profiles, thermal stability, and hypolimnetic oxygen depletion:
493 Implications for a warmer world. *Limnol. Oceanogr.* **51**(2): 815-819.
494 doi:10.4319/lo.2006.51.2.0815

495 Jöhnk, K. D., and others. 2008. Summer heatwaves promote blooms of harmful
496 cyanobacteria. *Glob. Change Biol.* **14**: 495-512. doi:10.1111/j.1365-
497 2486.2007.01510.x

498 Laird, N. F., and D. A. R. Kristovich. 2002. Variations of sensible and latent heat fluxes from
499 a Great Lakes buoy and associated synoptic weather patterns. *J. Hydrometeorol.* **3**: 3–
500 12

501 Le Moigne, P., J. Colin, and B. Decharme. 2016. Impact of lake surface temperatures
502 simulated by the FLake scheme in the CNRM-CM5 climate model. *Tellus* **68A**.
503 doi:10.3402/tellusa.v68.31274

504 Lenters, J. D., T. K. Kratz, and C. J. Bowser. 2005. Effects of climate variability on lake
505 evaporation: Results from a long-term energy budget study of Sparkling Lake,
506 northern Wisconsin (USA). *J. Hydrology* **308**: 168-195

507 Livingstone, D. M., A. F. Lotter, and I. R. Walker. 1999. The decrease in summer surface
508 water temperature with altitude in Swiss Alpine Lakes: A comparison with air
509 temperature lapse rates. *Arct. Antarc. Alp. Res.* **31**: 341-352. doi:10.2307/1552583

510 Livingstone, D. M. 2003. Impact of secular climate change on the thermal structure of a large
511 temperate central European lake. *Clim. Change* **57**(1): 205-225.
512 doi:10.1023/A:1022119503144

513 Lofgren, B. M., and Y. Zhu. 2000. Surface energy fluxes on the Great Lakes based on
514 satellite- observed surface temperatures 1992 to 1995. *J. Great Lakes Res.* **26**: 305–
515 314

516 Lofgren, B. M. 1997. Simulated effects of idealized Laurentian Great Lakes on regional and
517 large-scale climate. *J. Climate* **10**: 2847-2858

518 Lorenzetti, J. A., C. A. S. Araújo, and M. P. Curtarelli. 2015. Mean diel variability of
519 surface energy fluxes over Manso Reservoir. *Inland Waters* **5**: 155-172.
520 doi:10.5268/IW-5.2.761

521 MacIntyre, S., J. R. Romero, and G. W. Kling. 2002. Spatial-temporal variability in surface
522 layer deepening and lateral advection in an embayment of Lake Victoria, East Africa.
523 *Limnol. Oceanogr.* **47**: 656-671. doi:10.4319/lo.2002.47.3.0656

524 MacIntyre, S., and others. 2010. Buoyancy flux, turbulence, and the gas transfer coefficient in
525 a stratified lake. *Geophys. Res. Lett.* **37**(24). doi:10.1029/2010GL044164

526 McCormick, M. J. 1990. Potential changes in thermal structure and cycle of Lake Michigan
527 due to global warming. *T. Am. Fish. Soc.* **119**: 183-194

528 Momii, K., and Y. Ito. 2008. Heat budget estimates for Lake Ikeda, Japan. *J. Hydrol.* **361**:
529 362-370

530 Moukomla, S., and P. D. Blanken. 2017. The estimation of the North American Great Lakes
531 turbulent fluxes using satellite remote sensing and MERRA reanalysis data. *Remote*
532 *Sens.* **9**: 141. doi:10.3390/rs9020141

533 North, R. P., and others. 2014. Long-term changes in hypoxia and soluble reactive
534 phosphorus in the hypolimnion of a large temperate lake: consequences of a climate
535 regime shift. *Glob. Change Biol.* **20**: 811-823. doi:10.1111/gcb.12371

536 O'Beirne, M. D., J. P. Werne, R. E. Hecky., and others. 2017. Anthropogenic climate change
537 has altered primary productivity in Lake Superior. *Nat. Commun.* **8**: 15713.
538 doi:10.1038/ncomms15713

539 O'Reilly, C., and others. 2015. Rapid and highly variable warming of lake surface waters
540 around the globe. *Geophys. Res. Lett.* **42**: 10773-10781. doi:10.1002/2015GL066235

541 Peeters, F., and others. 2002. Modeling 50 years of historical temperature profiles in a large
542 central European lake. *Limnol. Oceanogr.* **47**: 186-197.
543 doi:10.4319/lo.2002.47.1.0186

544 Perroud, M., and S. Goyette. 2010. Impact of warmer climate on Lake Geneva water-
545 temperature profiles. *Boreal Environ. Res.* **15**: 255-278

546 Piccolroaz, S., and others. 2013. A simple lumped model to convert air temperature into
547 surface water temperature in lakes. *Hydrol. Earth Syst. Sci.* **17**: 3323-3338.
548 doi:10.5194/hess-17-3323-2013

549 Podgrajsek, E., E. Sahlée, and A. Rutgersson. 2015. Diel cycle of lake-air CO₂ flux from a
550 shallow lake and the impact of waterside convection on the transfer velocity. *J.*
551 *Geophys. Res. Biogeosci.* **120**: 29-38. doi:10.1002/2014jg002781

552 Polsenaere, P., et al. 2013. Thermal enhancement of gas transfer velocity of CO₂ in an
553 Amazon floodplain lake revealed by eddy covariance measurements. *Geophys. Res.*
554 *Lett.* **40**: 1734-1740. doi:10.1002/grl.50291

555 R Development Core Team. 2014. R: A language and environment for statistical computing,
556 R Foundation for Statistical Computing. Vienna, Austria. (Available at [http://www.R-](http://www.R-project.org/)
557 [project.org/.](http://www.R-project.org/))

558 Raymond, P. A., and others. 2013. Global carbon dioxide emissions from inland waters.
559 *Nature.* **503**: 355-359. doi:10.1038/nature12760

560 Read, J. S., and others. 2012. Lake-size dependency of wind shear and convection as controls
561 on gas exchange. *Geophys. Res. Lett.* **39**(9). doi:10.1029/2012GL051886

562 Riveros-Iregui, D. A., J. D. Lenters, C. S. Peake, J. B. Ong, N. C. Healey, and V. A. Zlotnik.
563 2017. Evaporation from a shallow, saline lake in the Nebraska Sandhills: Energy
564 balance drivers of seasonal and interannual variability. *J. Hydrology.* **553**: 172-187

565 Rose, K. C., K. C. Weathers, A. L. Hetherington, D. P. Hamilton. 2016. Insights from the
566 Global Lake Ecological Observatory Network (GLEON). *Inland Waters.* **6**: 476-482.
567 doi:10.5268/IW-6.4.1051

568 Rouse, W. R., and others. 2005. The role of northern lakes in a regional energy balance. *J.*
569 *Hydrometeor.* **6**: 291–305. doi:10.1175/JHM421.1

570 Rueda, F., E. Moreno-Ostos, and L. Cruz-Pizarro. 2007. Spatial and temporal scales of
571 transport during the cooling phase of the ice-free period in a small high-mountain
572 lake. *Aquat. Sci.* **69**: 115-128. doi:10.1007/s00027-006-0823-8

573 Samuelsson, P., E. Kourzeneva, and D. Mironov. 2010. The impact of lakes on the European
574 climate as simulated by a regional climate model. *Boreal Environ. Res.* **15**: 113-129

575 Schladow, S. G., and others. 2002. Oxygen transfer across the air-water interface by natural
576 convection in lakes. *Limnol. Oceanogr.* **47**(5): 1394-1404.
577 doi:10.4319/lo.2002.47.5.1394

578 Schmid, M., S. Hunziker, and A. Wüest. 2014. Lake surface temperatures in a changing
579 climate: a global sensitivity analysis. *Clim. Change* **124**: 301–315.
580 doi:10.1007/s10584-014-1087-2

581 Stainsby, E. A., and others. 2011. Changes in the thermal stability of Lake Simcoe from 1980
582 to 2008. *J. Great Lakes. Res.* **37**: 55-62. doi:10.1016/j.jglr.2011.04.001

583 Straskraba, M. 1980. The effects of physical variables on freshwater production: Analyses
584 based on models. p. 13-84. In E. D. LeCren (ed.). *The functioning of freshwater*
585 *ecosystems.* Cambridge Univ. Press

586 Thiery, W., and others. 2015. The impact of the African Great Lakes on the regional climate.
587 *J. Climate* **28**: 4061-4085. doi:10.1175/JCLI-D-14-00565.1

588 Vachon, D., Y. T. Prairie, and J. J. Cole. 2010. The relationship between near-surface
589 turbulence and gas transfer velocity in freshwater systems and its implications for
590 floating chamber measurements of gas exchange. *Limnol. Oceanogr.* **55**: 1723-1732.
591 doi:10.4319/lo.2010.55.4.1723

592 Verburg, P., and J. P. Antenucci. 2010. Persistent unstable atmospheric boundary layer
593 enhances sensible and latent heat loss in a tropical great lake: Lake Tanganyika. *J.*
594 *Geophys. Res.* **115**. doi:10/1029/2009JD012839

595 Verburg, P., R. E. Hecky, and H. Kling. 2003. Ecological consequences of a century of
596 warming in Lake Tanganyika. *Science* **301**: 505-507. doi:10.1126/science.1084846

597 Vörösmarty, C. J., and others. 2010. Global threats to human water security and river
598 biodiversity. *Nature* **467**: 555-561. doi:10.1038/nature09440

599 Vörösmarty, C. J., P. Green, J. Salisbury, and R. B. Lammers. 2000. Global water resources:
600 Vulnerability from climate change and population growth. *Science* **289**(5477): 284–
601 288. doi:10.1126/science.289.5477.284

602 Wang, W., X. Lee, W. Xiao, and others. 2018. Global lake evaporation accelerated by
603 changes in surface energy allocation in a warmer climate. *Nature Geoscience.*
604 Doi:10.1038/s41561-018-0114-8

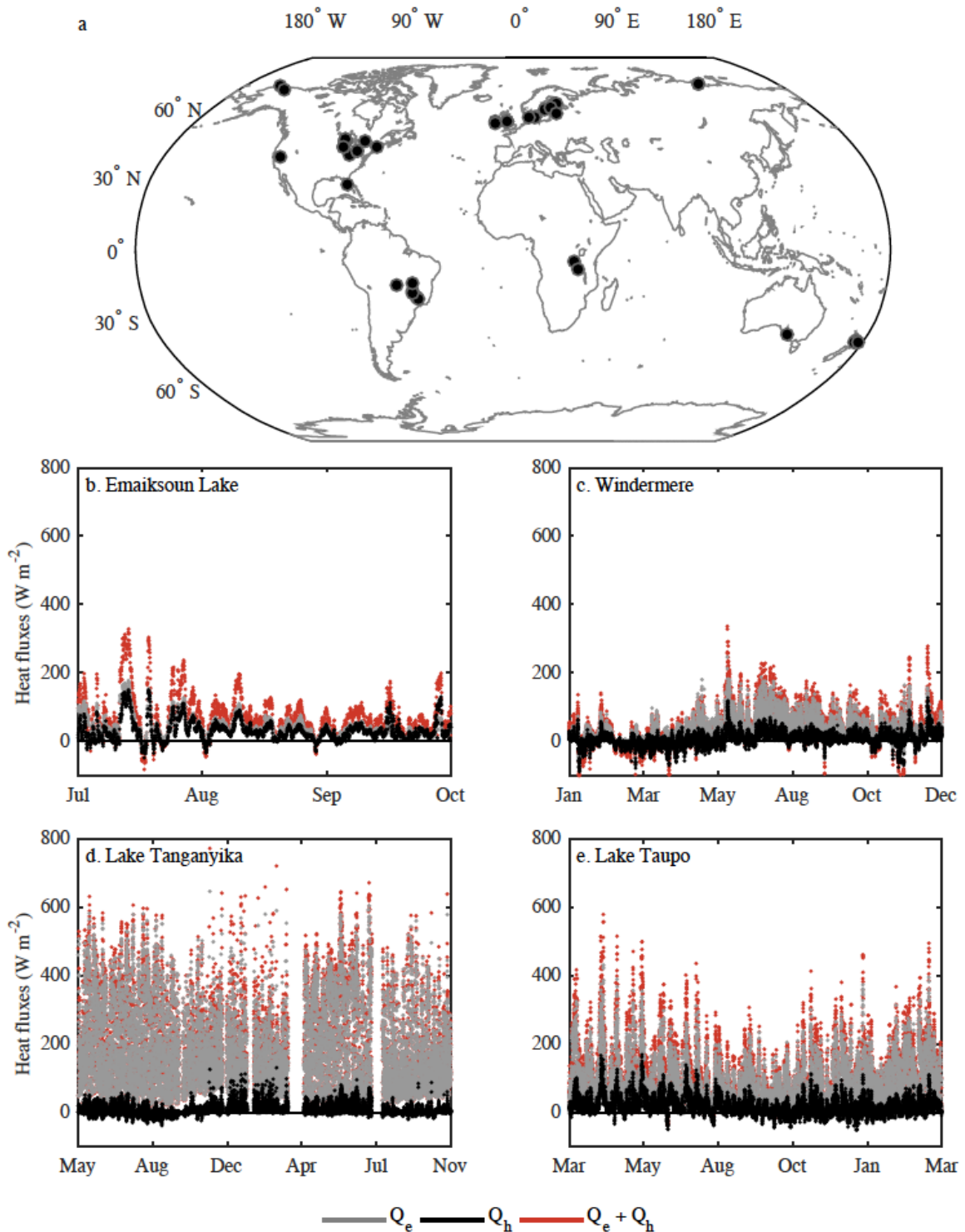
605 Wentz, F. J., and others. 2007. How much more rain will global warming bring? *Science* **317**:
606 233–235. doi:10.1126/science.1140746

607 Woolway, R. I., I. D. Jones, D. P. Hamilton, S. C. Maberly, K. Muraoka, J. S. Read, R. L.
608 Smyth, and L. A. Winslow. 2015a. Automated calculation of surface energy fluxes
609 with high-frequency lake buoy data. *Env. Mod. Soft.* **70**: 191–198.
610 doi:10.1016/j.envsoft.2015.04.013

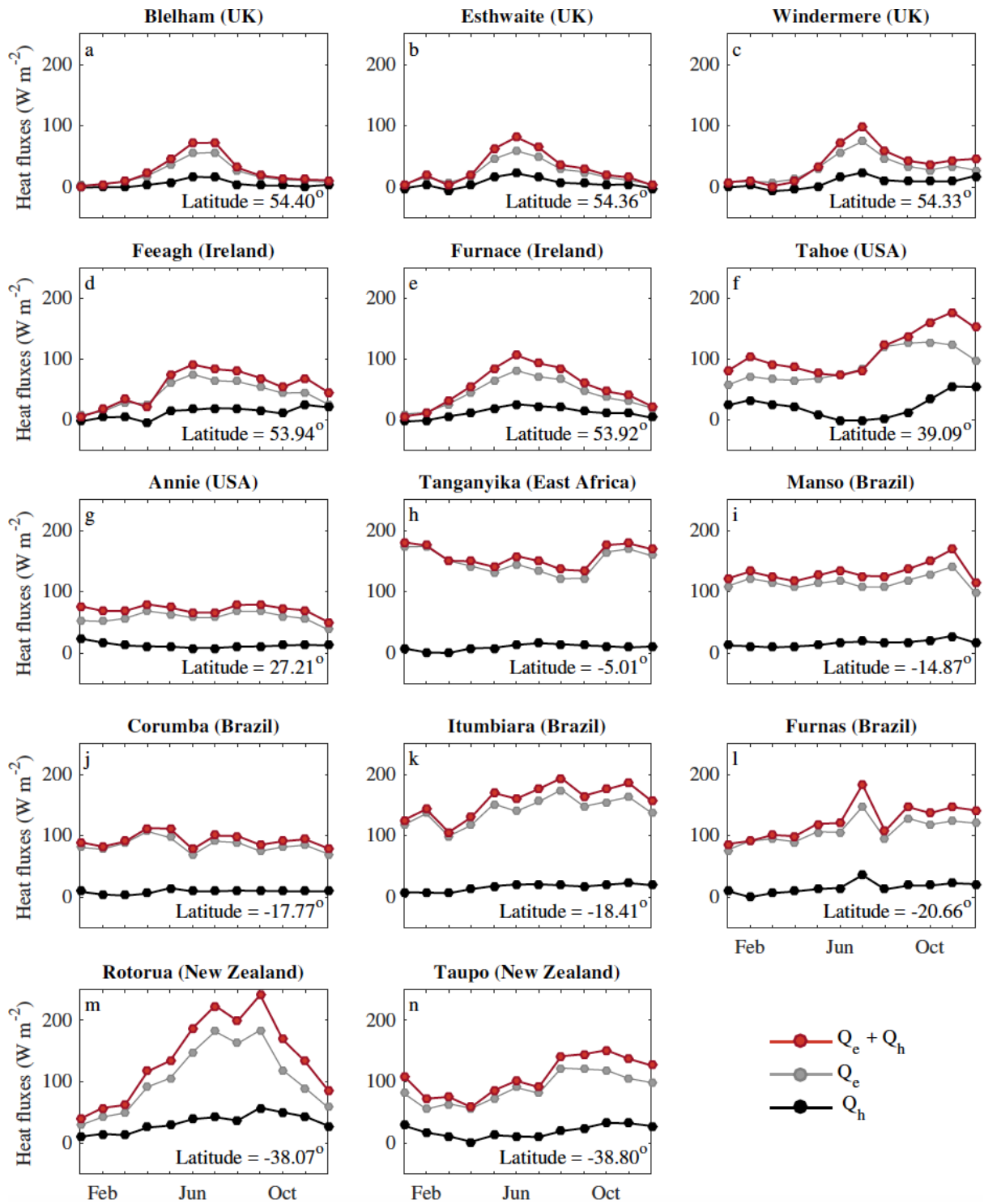
- 611 Woolway, R. I., I. D. Jones, H. Feuchtmayr, and S. C. Maberly. 2015b. A comparison of the
612 diel variability in epilimnetic temperature for five lakes in the English Lake District.
613 *Inland Waters* **5**: 139–154. doi:10.5268/IW-5.2.748
- 614 Woolway, R. I., and C. J. Merchant. (2017). Amplified surface temperature response of cold,
615 deep lakes to inter-annual air temperature variability. *Sci. Rep.* **7**(4130).
616 doi:10.1038/s41598-017-04058-0
- 617 Woolway, R. I., and others. 2017a. Latitude and lake size are important predictors of over-
618 lake atmospheric stability. *Geophys. Res. Lett.* **44**: 8875-8883.
619 doi:10.1002/2017GL073941
- 620 Woolway, R. I., and others. 2017b. Atmospheric stilling leads to prolonged thermal
621 stratification in a large shallow polymictic lake. *Clim. Change* **141**(4): 759-773.
622 doi:10.1007/s10584-017-1909-0
- 623 Woolway, R. I., and others. 2016. Diel surface temperature range scales with lake size. *PLoS*
624 *ONE* **11**(3): e0152466. doi:10.1371/journal.pone.0152466
- 625 Wu, P., N. Christidis, and P. Stott. 2013. Anthropogenic impact on Earth's hydrological
626 cycle. *Nat. Clim. Change* **3**: 807-810. doi:10.1038/nclimate1932
- 627 Wüest, A., and A. Lorke. 2003. Small-scale hydrodynamics in lakes. *Annu. Rev. Fluid Mech.*
628 **35**: 373-412. doi:10.1146/annurev.fluid.35.101101.161220

629 **Acknowledgements**

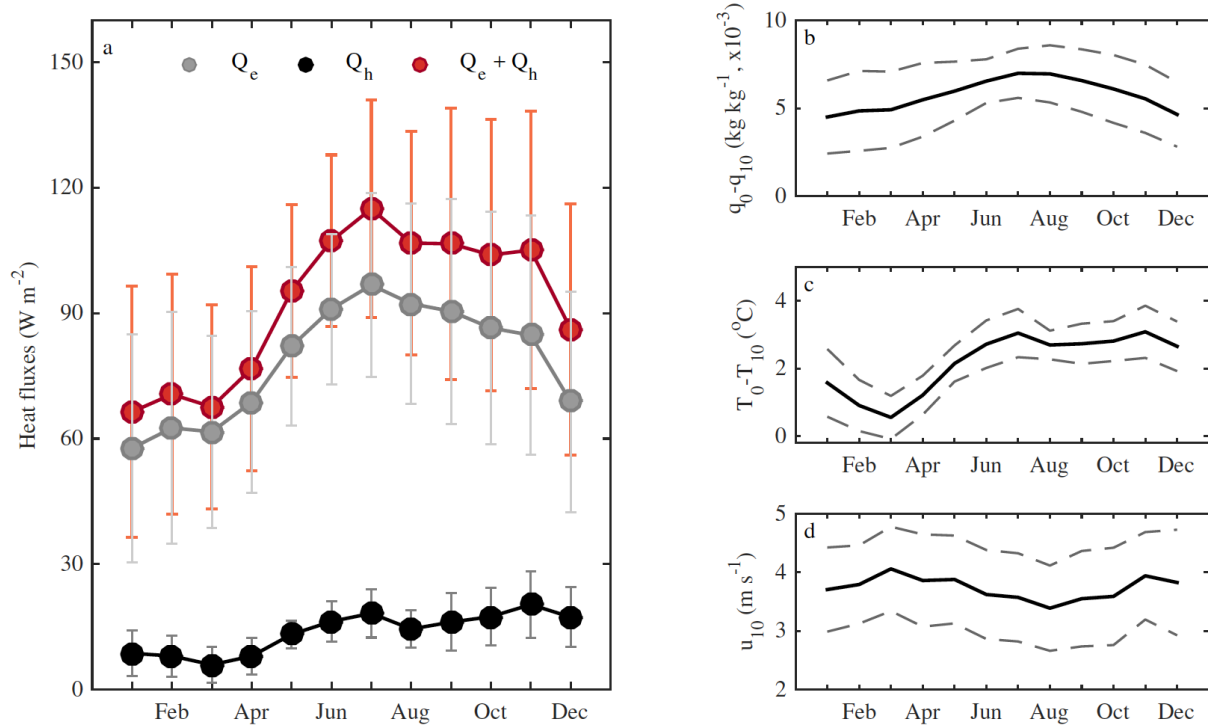
630 RIW was funded by EUSTACE (EU Surface Temperature for All Corners of Earth), which
631 received funding from the European Union's Horizon 2020 Programme for Research and
632 Innovation, under Grant Agreement no 640171. We thank individuals that contributed to the
633 collection of data included in this analysis: Jon Cole (Peter Lake); Ken Hinkel and Brittany
634 Potter (Emaiksoun Lake); Peter Staehr (Hampe Soe and Grib Soe); Hilary Swain (Lake
635 Annie). This work benefited from participation in the Global Lake Ecological Observatory
636 Network (GLEON) and the Networking Lake Observatories in Europe (NETLAKE). JAR
637 acknowledges funding from the Ontario Ministry of the Environment and Climate Change
638 and the Inter-American Institute for Global Change Research (Grant CRN3038). JDL was
639 supported by a grant from the National Science Foundation (NSF) Arctic Observing Network
640 (AON; grant number 1107792). Data collection for Lake Võrtsjärv was supported by the
641 Estonian Ministry of Education and Research, grant IUT21-2. The Centre for Ecology and
642 Hydrology, UK, funded data collection from the Cumbrian lakes. We thank Kevin Rose who
643 provided a helpful review of an early version of this work. Researchers from various
644 institutions provided data used this study. Please contact R. Iestyn Woolway
645 (riwoolway@gmail.com) for more information regarding requests for data from the relevant
646 individuals. We would like to thank two anonymous reviewers who provided a constructive
647 review of this manuscript.



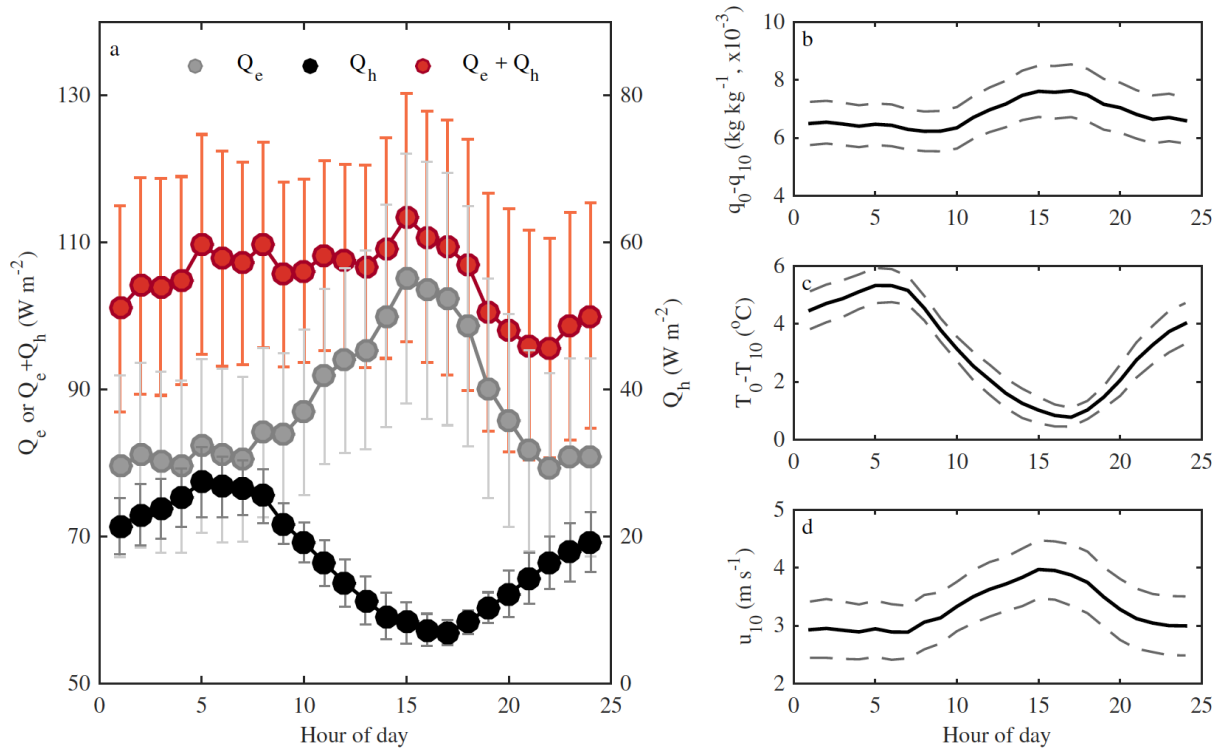
650
 651 **Figure 1.** (a) Locations of the 45 lakes in this study for which turbulent surface heat fluxes
 652 were estimated, and examples of calculated hourly latent (Q_e , gray), sensible (Q_h , black) and
 653 the sum of turbulent heat fluxes ($Q_e + Q_h$, red) at (b) Emaiksoun Lake (Alaska, USA;
 654 71.24°N, -156.78°E), (c) Windermere (United Kingdom; 54.35°N, -2.98°E), (d) Lake
 655 Tanganyika (south basin; East Africa; -8.47°N, 30.91°E), and (e) Lake Taupo (New Zealand;
 656 -38.80°N, 175.90°E). Positive values indicate cooling of the lake surface.



657
658 **Figure 2.** Monthly averaged latent (Q_e , gray), sensible (Q_h , black) and the sum of turbulent
659 heat fluxes ($Q_e + Q_h$, red) for 14 lakes with data available throughout the year. Lakes are
660 arranged by latitude from north to south. Southern hemisphere lakes were shifted by 182
661 days.
662



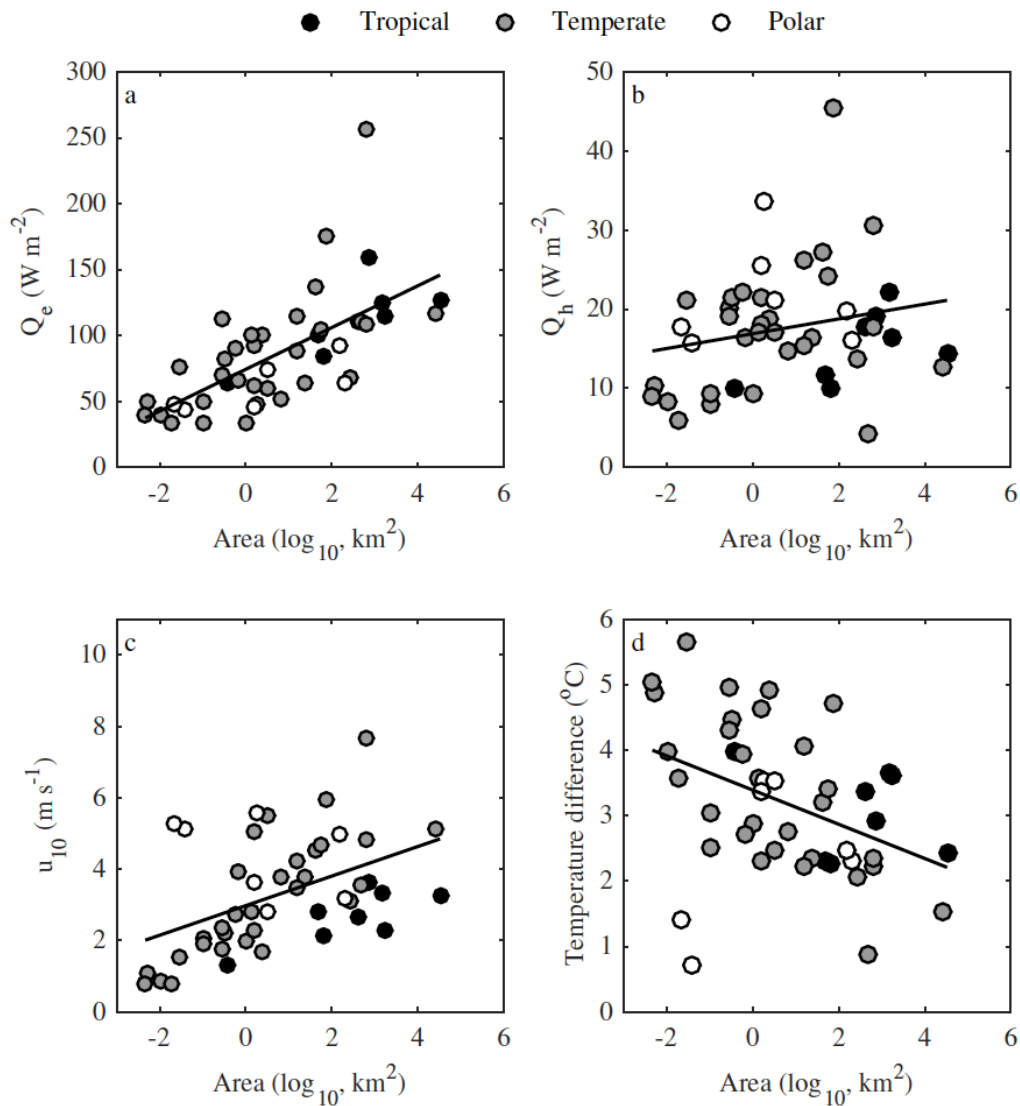
663
 664 **Figure 3.** Across-lake monthly averaged (a) latent (Q_e , gray), sensible (Q_h , black) and the
 665 sum of turbulent heat fluxes ($Q_e + Q_h$, red) at the water-air interface, (b) the water-air
 666 humidity difference, (c) the water-air temperature difference, and (d) the wind speed adjusted
 667 to a height of 10 m (u_{10}). Averages are shown for 14 lakes with data available throughout the
 668 year (as shown in Fig. 2). The 95% confidence intervals are also shown.
 669



671

672 **Figure 4.** Across-lake summer (July-September in northern hemisphere and January-March
 673 in southern hemisphere) average diel cycles of (a) latent (Q_e , gray), sensible (Q_h , black) and
 674 the sum of turbulent heat fluxes ($Q_e + Q_h$, red) at the water-air interface, (b) the water-air
 675 humidity difference, (c) the water-air temperature difference, and (d) the wind speed adjusted
 676 to a height of 10 m (u_{10}). Averages are shown for 45 lakes. The 95% confidence intervals are
 677 also shown.

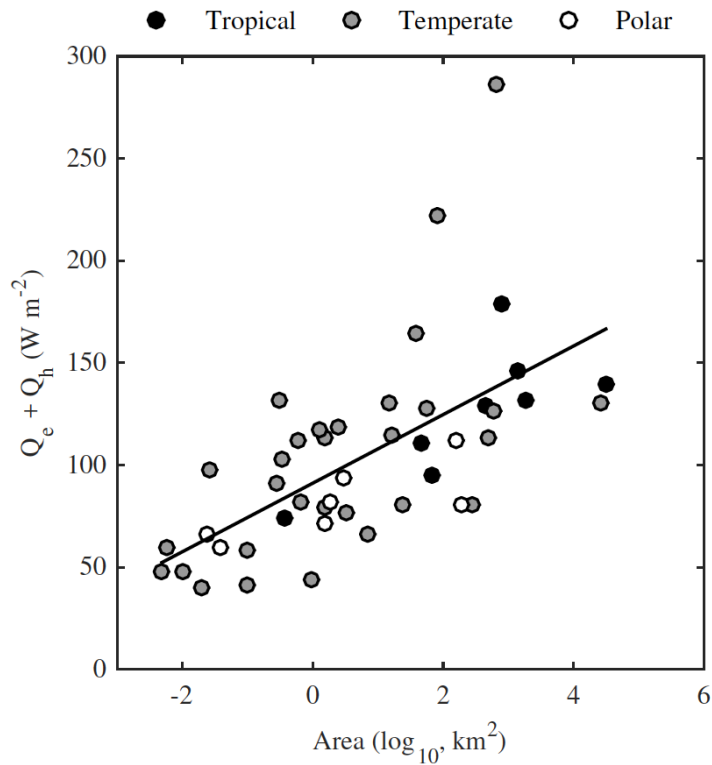
678



679

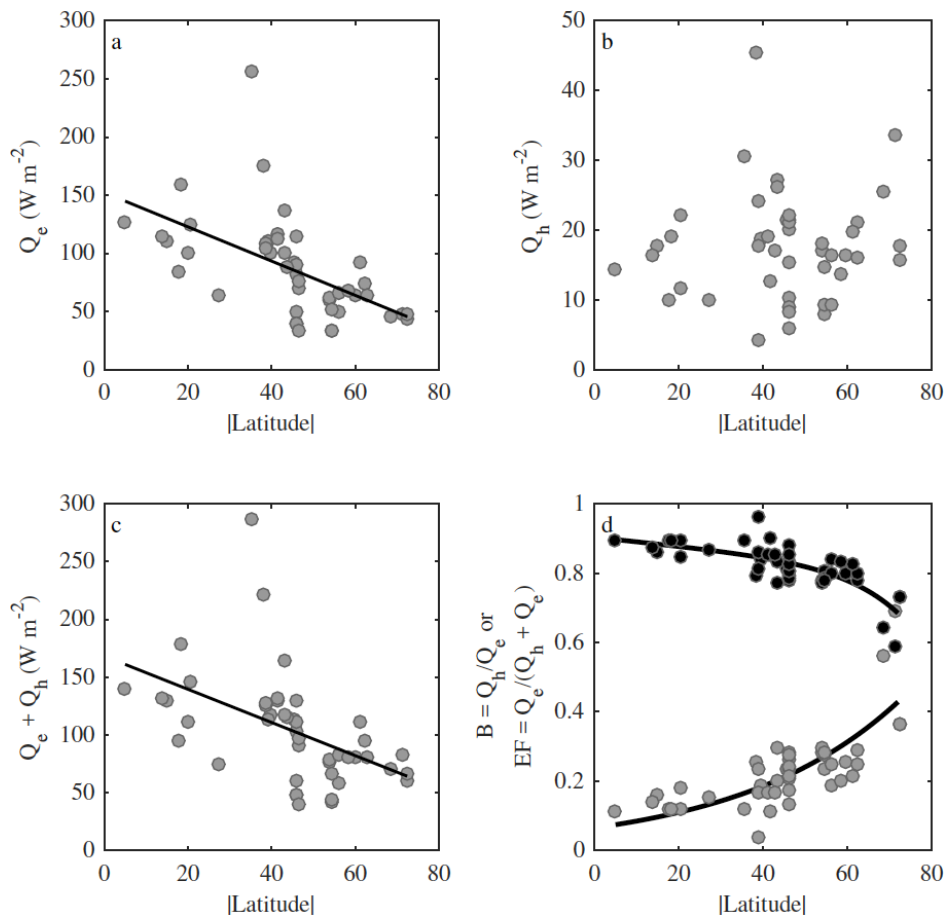
680 **Figure 5.** Relationship between lake surface area (\log_{10}) and summer-mean (July-September
 681 in northern hemisphere and January-March in southern hemisphere) (a) latent (Q_e) and (b)
 682 sensible (Q_h) heat fluxes, (c) surface wind speeds adjusted to a height of 10 m (u_{10}), and (d)
 683 the water-air temperature difference across 45 lakes. Points are colored according to climatic
 684 zones, which are defined by the absolute latitude of each lake: tropical ($<30^{\circ}$, black),
 685 temperate ($30\text{-}60^{\circ}$, gray), and polar ($>60^{\circ}$, white). Statistically significant ($p < 0.05$) linear
 686 fits to the data are shown.

687



688
 689
 690
 691
 692
 693
 694
 695

Figure 6. Relationship between lake surface area (\log_{10}) and summer-mean (July-September in northern hemisphere and January-March in southern hemisphere) sum of turbulent heat fluxes ($Q_e + Q_h$) at the water-air interface across 45 lakes. Points are colored according to climatic zones, which are defined by the absolute latitude of each lake: tropical ($<30^\circ$, black), temperate ($30-60^\circ$, gray), and polar ($>60^\circ$, white). A statistically significant ($p < 0.05$) linear fit to the data is shown.



696

697 **Figure 7.** Relationship between latitude (shown as absolute latitude) and (a) latent (Q_e), (b)

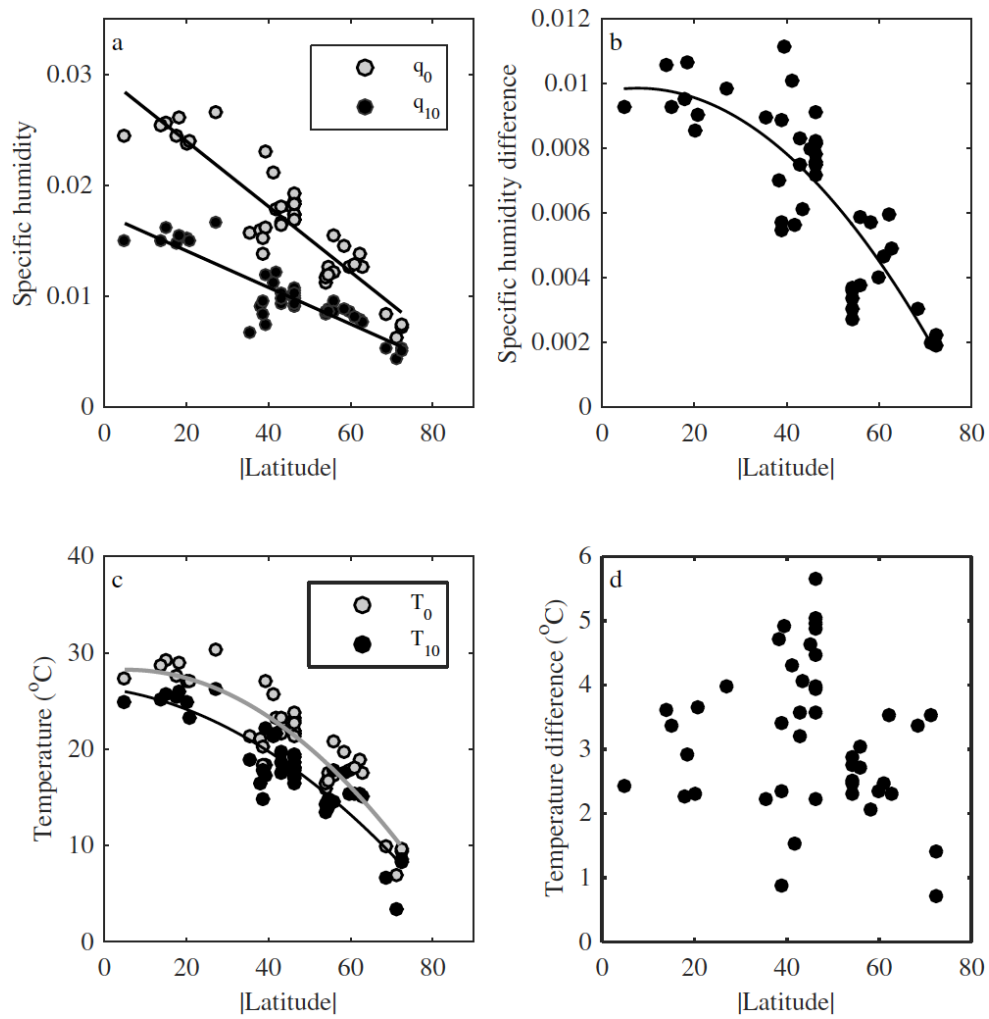
698 sensible (Q_h) and (c) the sum of turbulent heat fluxes ($Q_e + Q_h$) at the water-air interface, and

699 (d) the ratio of the summer-mean Q_h to summer-mean Q_e ($B = Q_h/Q_e$; gray), and the relative

700 contribution of summer-mean Q_e to the summer-mean total turbulent heat flux

701 ($EF = Q_e/(Q_h + Q_e)$; black). Statistically significant ($p < 0.05$) linear fits to the data are shown,

702 except for Fig. 7d where an exponential relationship is shown.



703

704 **Figure 8.** Relationship between latitude (shown as absolute latitude), and (a) the specific
 705 humidity above the lake surface (q_{10} ; black) and at saturation (q_s ; gray); (b) the specific
 706 humidity difference ($q_s - q_{10}$); (c) mean surface air temperature (T_{10} ; black) and lake surface
 707 temperature (T_0 ; gray); (d) the temperature difference at the water-air interface ($T_0 - T_{10}$).
 708 Relationships are shown for summer (July-September in northern hemisphere and January-
 709 March in southern hemisphere) means across 45 lakes. Statistically significant ($p < 0.05$)
 710 linear fits to the data are shown, except for Figs 8b and 8c where an exponential relationship
 711 is shown.